

Patch-Based Deep Unsupervised Image Segmentation using Graph Cuts

Isaac Wasserman
University of Pennsylvania
Philadelphia, Pennsylvania
isaacrw@seas.upenn.edu

Jeová Farias Sales Rocha Neto
Bowdoin College
Brunswick, Maine
j.farias@bowdoin.edu

Abstract

Unsupervised image segmentation aims at grouping different semantic patterns in an image without the use of human annotation. Similarly, image clustering searches for groupings of images based on their semantic content without supervision. Classically, both problems have captivated researchers as they drew from sound mathematical concepts to produce concrete applications. With the emergence of deep learning, the scientific community turned its attention to complex neural network-based solvers that achieved impressive results in those domains but rarely leveraged the advances made by classical methods. In this work, we propose a patch-based unsupervised image segmentation strategy that bridges advances in unsupervised feature extraction from deep clustering methods with the algorithmic help of classical graph-based methods. We show that a simple convolutional neural network, trained to classify image patches and iteratively regularized using graph cuts, naturally leads to a state-of-the-art fully-convolutional unsupervised pixel-level segmenter. Furthermore, we demonstrate that this is the ideal setting for leveraging the patch-level pairwise features generated by vision transformer models. Our results on real image data demonstrate the effectiveness of our proposed methodology.

1. Introduction

Image segmentation has long been one of the main tasks in computer vision and it has been widely applied in general image understanding or as a preprocessing step for other tasks such as object detection. It aims at corresponding each pixel in an image to a semantically relevant class, in such a way that similar pixels are assigned to the same class. This problem finds various industrial applications such as autonomous driving, medical image analysis, video surveillance and virtual reality to name a few [32].

On the supervised front, deep learning approaches using Convolutional (CNN) and Fully Convolutional Neural Networks (FCN) achieved unprecedented results in image seg-

mentation, as illustrated by the UNet [37] and DeepLab [13] models. Recently, however, methods using transformer-based models, such as Segformer [46], DETR [9] and DINO [11], are slowly outperforming established CNN solutions. This has prompted the recent interest in deep models that utilize image patches instead of their full-sized counterparts [22,41], leading some to postulate that patch representations are the main source of the transformer’s success [42].

These accomplishments come, however, at the cost of long training schemes and the need for larger amounts of annotated data, which hinder their application in many domains where data can be expensive or scarce, such as in biology, or astrophysics [47]. These issues can be resolved via the application of unsupervised techniques instead. In this setting, one aims at creating a model that automatically discovers semantically important visual features or groups that characterize the various objects in a scene. Classically, this could be approached via variational, statistical, and graphical methods, exemplified in active contours [12], conditional random fields [27], and graph cuts [7,39]. Within the deep learning literature, prominent advances were made in the field of unsupervised deep image clustering [36], which eventually led to developments in deep image segmentation techniques [20,21,25,30,44].

In this work, we introduce GraPL, an unsupervised image segmentation technique that draws inspiration from the success of CNNs for imaging tasks, the learning strategies of deep clustering methods, and the regularization power of graph cut algorithms. Here, we alternate the training of a CNN classifier on image patches and the minimization of a clustering energy via graph cuts. To the best of our knowledge, this is the first attempt in both the deep clustering and image segmentation literature to make use of graphs cuts to solve a deep learning-based unsupervised task. We show that our zero-shot approach detects visual segments in an image without onerous unsupervised training on an entire image dataset, automatically finds a satisfactory number of image segments, and easily translates the patch-level training to efficient pixel-level inference. Furthermore, because of its structure, it also naturally incorpo-

rates pretrained patch embeddings [11, 33], without relying on them for the final product. Finally, we show that this simple approach achieves state-of-the-art results in deep unsupervised image segmentation, demonstrating the potential of graph cuts to improve other patch-based deep segmentation algorithms. Specifically, we make the following main contributions with our work:

- We introduce GraPL, an unsupervised segmentation method that learns a fully convolutional segmenter directly from the image’s patches, using an iterative algorithm regularized by graph cuts.
- We show that this framework naturally employs patch embeddings for pixel-level segmentation without the need for postprocessing schemes such as CRF refining.
- We demonstrate that GraPL is able to outperform the state-of-the-art in deep unsupervised segmentation by iteratively training a small, low complexity CNN.

2. Related Work

2.1. Deep Clustering

With the advancements in deep supervised image classification techniques, interest in deep architectures to solve unsupervised problems followed naturally. This pursuit led to the task of partitioning image datasets into clusters using deep representations without human supervision, inaugurating the body of work which is now referred to as “deep clustering.” The interested reader is referred to [36] for a comprehensive review on the available approaches to deep clustering.

In GraPL, we treat image patches as individual images to be clustered as a pretext task to train our segmenter and efficiently use graph cuts to impose constraints on the patch clusters. To the best of our knowledge, our method is the first to use MRF-based algorithms for clustering CNN-generated visual features.

2.2. Deep Unsupervised Image Segmentation

As deep clustering aims to learn visual features and groupings without human annotation via deep neural models, deep unsupervised image segmentation hopes to use the same models to learn coherent and meaningful image regions without the use of ground-truth labels. To do so, many methods explore strategies that resemble those from deep clustering. Cho *et al.* [15] iteratively employs k -means to cluster pixel-level features extracted from a network trained on different photometrically and geometrically varying image views. The work in [24] efficiently extends a mutual information-based deep clustering algorithm to the pixel-level by recognizing that such a process can be achieved via convolution operations. [23] computes pixel embeddings from a metric learning network and segments each image using a spherical k -means clustering algorithm.

In [25], the authors train an FCN with pseudo-labels generated by the same network in a prior step. They attain reliable segmentations by proposing a complex loss function that ensures the similarity among pixels in shared segments, while encouraging their spacial continuity and limiting their total count. Our method, while similarly training an FCN, works on patches and is able to reinforce spacial continuity and low segment count via our graph cut approach. Furthermore, due to its use of graph cuts, GraPL is able to naturally incorporate pairwise patch relationships. Finally, while other patch-based unsupervised solutions require a segmentation refinement stage after a patch feature clustering step [21, 43, 44], we both discover and instill patch knowledge interactively, without the need for postprocessing our result.

2.3. Graph Cuts for Image Segmentation

Modeling image generation as a Markov random field (MRF) has a long history in Computer Vision, dating its initial theoretical and algorithmic achievements to the works of Abel *et al* [1] and Besag [5]. Soon enough, MRFs found applications in various image processing tasks, such as edge detection, image denoising, segmentation, and stereo [28]. In particular, the works conducted by Boykov and Jolly [7] and Boykov *et al.* [6] demonstrated that one can apply efficient min st -cut based algorithms to solve image segmentation by modeling it as a Maximum *a Posteriori* (MAP) estimator of an MRF. Their groundbreaking results made possible the emergence of classical graph-based segmentation methodologies such as GrabCut [38] and was, more recently, used to improve the training of CNN-based segmenters [31]. CRF modeling, closely related to MRF, has also played an important role in refining coarse network predictions in recent segmentation methods [13, 14, 48].

In some ways, our proposed method draws inspirations from the methodologies proposed by Rother *et al.* [38], and Marin *et al.* [31]. In [38], the authors propose GrabCut, an algorithm that iteratively bound-optimizes a segmentation energy, requiring the solution of a min st -cut problem at each iteration in order to perform unsupervised regularized fitting of the image’s appearance, which is modeled as a Gaussian mixture model. Our algorithm also uses min st -cut solvers iteratively, but here we (1) work on patch data, instead of individual pixels, and (2) fit the image appearance using a CNN classifier. Due to the nature of CNNs, our network can seamlessly translate the patch-level classifier into a pixel-level image segmenter. In [31], the authors show how to perform weakly-supervised CNN segmentation via an optimizer that alternates between solving an MAP-MRF problem and gradient computation. In contrast, our method solves a fully unsupervised segmentation problem and does not use our MAP solution to adjust gradient directions.

3. Methodology

GraPL (Graph Cuts at the Patch Level) is a fully unsupervised segmentation method which operates in a single-image paradigm. Using patch clustering as a pretext task for segmentation, during training it is able to learn distinctive segment features that enable it to effectively segment the image at the pixel level. Although other techniques have previously shown patch clustering to be an effective surrogate task [24, 34, 43, 44], our method demonstrates that clustering the patches of a single image provides sufficient feature learning to accurately segment it. GraPL’s training is guided by patch-level graph cuts; this intervention imposes spatial coherence priors which are helpful for learning clusters that are conducive to segmentation. At inference, the complexities of the pipeline disappear, leaving only the network. Leveraging a generalization of CNNs, the trained model is “convolved” over the entire image to produce a pixel-level segmentation.

3.1. Algorithm

Let $I : \Omega \mapsto \mathbb{R}^c$ be an image of c channels with pixel set $\Omega = \{1, \dots, n\} \times \{1, \dots, m\}$, and $S : \Omega \mapsto \{1, \dots, K\}$ be a segmentation map of I in K regions. Let \mathcal{P} be a set of patches from I , such that all patches are of the same size, i.e., for each p in \mathcal{P} , $p : \Omega_p \mapsto \mathbb{R}^c$, $\Omega_p \subset \Omega$, $|\Omega_p| = \text{const}$. In practice, we populate \mathcal{P} by selecting all patches on a non-overlapping $d \times d$ grid of I , resulting in patches of shape $(w/d, h/d)$. We make this choice of \mathcal{P} based on two factors: (1) efficiency, as this operation can be efficiently performed by most deep learning libraries via their unfolding methods, and (2) simplicity, as it’s one of the simplest ways to generate equal sized patches that span Ω .

Let $F_\theta : \Omega \mapsto [0, 1]^{K \times |\Omega|}$ be an FCN, and $F'_\theta : \Omega_p \mapsto [0, 1]^K$ be a CNN patch classifier. In GraPL, both networks are parametrized by the same parameters θ . F'_θ is used in our training stage and is applied to the patches in \mathcal{P} , while F_θ is employed in our inference phase and is our final segmenter. The full algorithm is shown in Figure 1.

Training Stage Our goal is to learn θ exclusively from the data in \mathcal{P} and transfer it to F_θ . To do so, our method trains F'_θ by minimizing an energy formulated at the patch level of I . Let $S' : \mathcal{P} \mapsto \{1, \dots, K\}$ be a labeling for the patches in \mathcal{P} . Following the literature on MRF modeling [7], we define the energy of S' for an unknown θ as:

$$E(S', \theta | \mathcal{P}) = U(S', \theta | \mathcal{P}) + \lambda V(S' | \mathcal{P}), \quad (1)$$

with $\lambda \geq 0$. The unary term $U(\cdot)$ is traditionally defined as:

$$U(S', \theta | X) = - \sum_{p \in \mathcal{P}} \sum_{k=1}^K \mathbb{1}(S'(p) = k) [\ln F'_\theta(p)]_k, \quad (2)$$

where $\mathbb{1}(\cdot)$ is the indicator function and $[\cdot]_k$ is the k -th position of a vector. Let α and β be probability distributions in \mathbb{R}^K , and let $H(\alpha, \beta) = - \sum_{k=1}^K [\alpha]_k \ln [\beta]_k$ be their cross entropy. This means that Eq. 2 can be seen as the sum of cross entropies $H(S'(p), F'_\theta(p))$ between $S'(p)$, taken as a one-hot probability distribution, and $F'_\theta(p)$ over all $p \in \mathcal{P}$. The pairwise energy term $V(\cdot)$ is given by:

$$V(S' | \mathcal{P}) = \sum_{(p,q) \in \mathcal{P} \times \mathcal{P}} \mathbb{1}(S'(p) \neq S'(q)) \phi(p, q), \quad (3)$$

with the patch similarity function $\phi(\cdot)$ defined as:

$$\phi(p, q) = \frac{1}{\text{dist}(p, q)} \exp\left(-\frac{\text{aff}(p, q)^2}{2\sigma}\right), \quad (4)$$

where the data affinity function $\text{aff}(p, q)$ evaluates the data similarity between p and q , and $\text{dist}(p, q)$ considers the Euclidean distance between the centers of p and q . We select σ as the standard deviation of affinities for all $p, q \in \mathcal{P}$. To compute patch affinities we make use of a patch encoder, which extracts an embedding from each patch in \mathcal{P} .

Inspired by GrabCut [38], GraPL minimizes E using a block-coordinate descent iterative strategy, where we alternate between optimizing for θ and S' , keeping the other constant. The current labeling S'_t is updated using the current network parameters θ_{t-1} , now taken as fixed in Eq. 1:

$$S'_t = \arg \min_{S'} E(S' | \theta_{t-1}, \mathcal{P}). \quad (5)$$

The above problem can be approximately solved by a series of minimum st -cut in the form of α -expansion or $\alpha\beta$ -swap moves [6]. This step is can be quickly accomplished due to the efficiency of such graph cut algorithms and the comparatively small size of \mathcal{P} , which presents a further advantage to our patch-based framework. We then compute the updated parameters θ_t via:

$$\theta_t = \arg \min_{\theta} \mathcal{L}(F'_\theta(\mathcal{P}), S'_t), \quad (6)$$

where $F'_\theta(\mathcal{P}) = \{F'_\theta(p)\}_{p \in \mathcal{P}}$. We employ traditional gradient descent-based backpropagation to solve the above problem. The loss $\mathcal{L}(\cdot)$, is designed to predict the outputs of F'_θ on each patch using the labels from S'_t . Keeping S'_t fixed, Eq. 2 conveniently formulates that process as a sum of cross entropy losses, just as one would naturally devise in a supervised segmentation learning scheme. We then follow Kim *et al.* [25] and include a patch-level continuity loss $C(\theta)$:

$$C(\theta) = \sum_{p \in \mathcal{P}} \sum_{q \in \mathcal{N}_p} |F'_\theta(p) - F'_\theta(q)|, \quad (7)$$

where $|\cdot|$ is the $L1$ norm and \mathcal{N}_p is the set of patches immediately neighboring p in Ω space. In the general case, one can employ a k -nearest neighbors graph of the elements in \mathcal{P} , considering the Euclidean distance between patch cen-

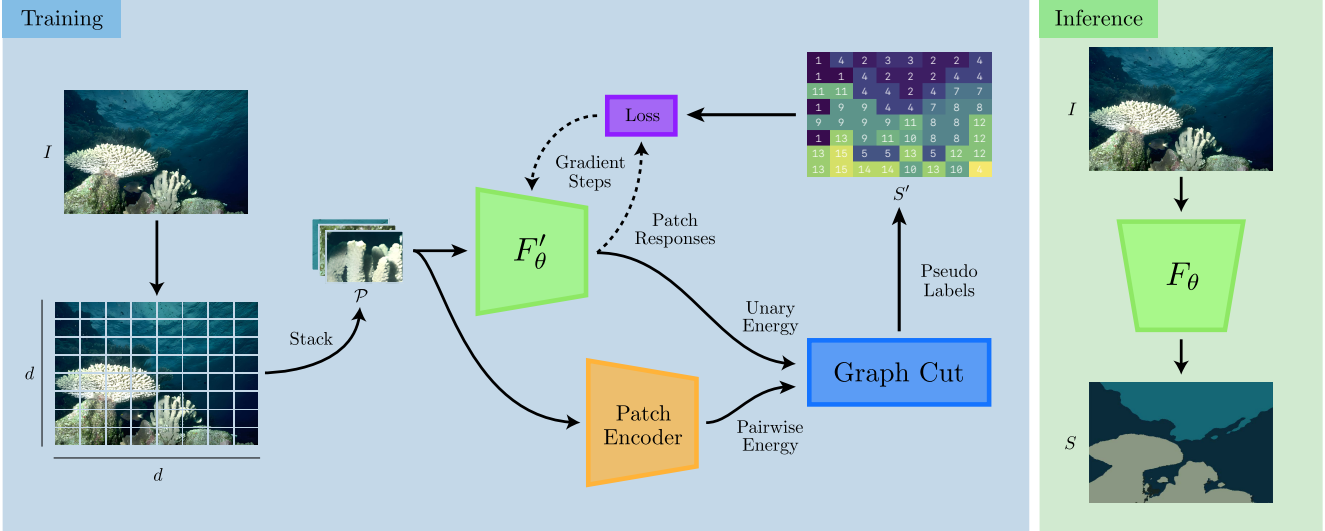


Figure 1. The proposed algorithm. GraPL trains a convolutional neural network to cluster patches of a single image without supervision under the guidance of graph cuts, spatial continuity loss, and a patch affinity encoder. At inference, this patch clustering knowledge is applied to pixel-level segmentation of the image. F'_θ and F_θ share the same parameters.

ters. For the $d \times d$ grid from Figure 1, we choose \mathcal{N}_p to be given by the patches immediately above and to the left of p , resembling what is done in [25]. This continuity loss brings spatial coherence outside the graph step and encourages smooth boundaries on the network outputs. In practice, we found it to be beneficial to have both the graph step and $C(\theta)$ in our method. Our final loss is then defined as:

$$\mathcal{L}(F'_\theta(\mathcal{P}), S'_{t-1}) = \sum_{p \in \mathcal{P}} H(S'_{t-1}(p), F'_\theta(p)) + \mu C(\theta), \quad (8)$$

where $\mu \geq 0$. As a consequence of the use of both graph cuts and the continuity loss described above, GraPL naturally suppresses extraneous labels arising from irrelevant patterns or textures, automatically promoting model selection.

As the alternation continues, F'_θ improves to the point where it no longer requires the guidance of the graph cuts to produce spatially and semantically coherent patch clusters. At that point, we end our training phase.

Inference Stage Once F'_θ is trained, our next goal is to classify all possible patches in I of shape equal to the patches in \mathcal{P} . To that end, we first assume that, as a CNN, F'_θ is composed of an initial series of convolutional layers and a final stage of say Q dense layers, along with a softmax function at the end. Assume that the inputs of all layers are unpaddinged, and that each dense layer has s_q units leading to a final output of size K . Now, one can replace each dense layer in F'_θ with a convolutional one of kernel size $\sqrt{s_q}$ and retain its exact functionality. Our resulting FCN, F_θ , is now capable of efficiently being applied to I , by ef-

fectively “convolving” it with patch classifier F'_θ .

3.2. Advantages of using Graph Cut Iterations

In the absence of labels, GraPL learns to cluster patches via an iterative procedure. This general formulation allows us to inject knowledge about the domain by designing an apt method for selecting pseudo-labels. While similar methods use k -means [10], mixture models [23], or simply argmax [25] to transform network outputs into new pseudo-labels, GraPL uses these response vectors to define the unary energy of a patch-level MRF graph of the image.

This approach for patch clustering introduces some advantages to our method. First, while the MRF modeling step is done primarily to impose a spatial coherence prior, due to the known shrinking bias of graph cuts [26], the resultant partition also smooths segment boundaries and reduces the number of distinct segments, leading to natural model selection. The spatial regularization introduced by the proposed graph can also be generalized to accommodate other classical graph formulations that consider segmentation seeds [6], appearance disparity [40], curvature [16], or target distributions [4]. Finally, in contrast to methods that discover objects by clustering patch embeddings arising from pre-trained transformers and applying a segmentation head [21] or CRF refinement [43, 44], GraPL considers patch embeddings only as way to guide its training stage, yielding a final pixel-level segmentation map without postprocessing. We consider our graph cut-based approach to handle rich patch features beneficial, as we do not overly depend on their clustering power, and simply reference them as guidance when regularizing our training.

4. Experiments

4.1. Implementation and Experimental Setup

Segmentation Task To evaluate the performance and behaviors of GraPL, the algorithm was tasked with segmenting the 200 image test set of BSDS500 [3] using a variety of hyperparameters. Segmentation performance is measured in terms of mean intersection over union (mIoU) [19], with predicted segments matched one-to-one with target segments using a version of the Hungarian algorithm modified to accommodate $\hat{K} \neq K^*$, where \hat{K} is the number of distinct segments in the final segmentation, and K^* is the number of segments in the ground truth. Results are averaged across 10 different random seeds for initialization.

Hyperparameters Unless otherwise specified, the following configuration was used during testing. Pseudo-labels were initialized according to the SLIC [2] based algorithm described in Section 4.2. GraPL was run for four training iterations, and the number of gradient steps in the loss minimization at each iteration was 40, 32, 22, and 12 respectively. K_0 , the number of initial segments was set at 14, and d was set to 32. Graph cuts were implemented using pyGCO [29], and the pairwise energy coefficient, λ , was set to 64. The continuity loss was assigned a weight of $\mu = 3$. The L_2 norm between DINOv2 [33] (ViT-L/14 distilled) patch embeddings was used as an affinity metric to determine pairwise weights.

Network Architecture An intentionally minimal CNN architecture was used, consisting of 2×3 unpadded convolutional layers with 32 and 8 filters, respectively. In F'_θ , this is followed by a dense classification head with K_0 units, and in F_θ it is followed by a $(\frac{h}{d} - 4) \times (\frac{w}{d} - 4)$ convolutional segmentation head with K_0 filters. The network layers are each separated by batch normalization, tanh activations, and dropout with rate 0.2. Without padding, our network is subject to certain regularization implications. In CNNs, zero padding an image has the effect of dropping out some of the weights of the subsequent convolutional layer. As our method requires the training phase to be executed on unpadded images, it is effectively deprived of this regularization feature. We found that applying dropout before the first convolutional layer all but resolved issues arising from the network’s lack of padding. Despite its simplicity, this network is complex enough to achieve reliable segmentations, and more complex networks did not lead to better performance. In our work, we also abstain from using padding on our inference phase, which results in $\hat{S} = F_\theta(I)$ being of a size smaller than Ω , due to the convolution operations in F_θ . GraPL handles this discrepancy by interpolating \hat{S} to the original dimensions via nearest neighbor interpolation. Networks were implemented using PyTorch 2.0.1 [35].

Early Stopping If a cross entropy loss of less than 1.0 was reached during the first iteration, it was stopped early, and new pseudo-labels were assigned. During the first iteration, we are fitting the initial pseudo-labels, which are either arbitrary or assigned by SLIC. By imposing this early stopping condition, we are avoiding the local minima where GraPL may be overfitting to a less performant (or worse, arbitrary) segmentation.

4.2. Ablation Studies

Initialization As an iterative algorithm, proper initialization is an important factor in training GraPL. Although similar deep clustering algorithms have used randomly initialized pseudo-labels [10, 25], we were unsure whether ignoring more principled approaches was leaving performance on the table. To answer this question, we compared four initialization strategies: “patchwise random,” “seedwise random,” “spatial clustering,” and an approach based on SLIC [2]. The “patchwise random” approach individually assigns each patch p in \mathcal{P} a random label. In the “seedwise random” strategy, we select K_0 random patches and assign them each one of the K_0 labels; the remaining patches are assigned the label of the patch closest to them. For “spatial clustering,” patches are clustered using k -means according to their (x, y) spatial coordinates to form K_0 clusters of roughly equal size. In the SLIC-based approach, we unfold a K_0 cluster SLIC segmentation with low compactness into the same patches as the input image. The on-hot labels of these patches are averaged and normalized to produce soft labels. These soft initializations are an attempt to regularize and retain all salient features of the patch during training.

Tests demonstrated that patchwise random initialization is not an ideal choice for GraPL (Table 1). This is likely because it encourages a disregard for spatial coherence during the first and most important iteration. While SLIC was shown to be the best choice out of the methods tested, seedwise random and spatial clustering initialization performed only 1.0% and 0.6% worse, respectively, and the algorithm could likely be tuned such that they meet or exceed the performance of SLIC. However, in the current configuration,

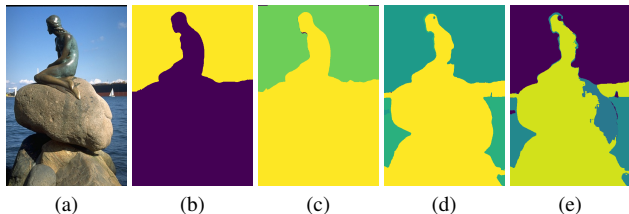


Figure 2. Example of undersegmentation from non-SLIC initialization. (a) Input image. (b) Patchwise Random ($\hat{K} = 2$). (c) Seedwise Random ($\hat{K} = 4$). (d) Spatial Clustering ($\hat{K} = 4$). (e) SLIC ($\hat{K} = 6$).

we notice a tendency for both of these methods to result in undersegmentation, in which $\Delta K = K_0 - \hat{K}$ is considerably higher than the SLIC version (Figure 2).

Pairwise Edge Weights The pairwise energy function (Eq. 4) used by GraPL includes an affinity function $\text{aff}(p, q)$. Designed with vision transformers in mind, this function is defined by the Euclidean distance between some patch metric or embedding $m(p)$ for $p \in \mathcal{P}$.

Though DINOv2 [33] has been shown to produce excellent, fully unsupervised features on the patch level, requiring minimal supervised fine-tuning to produce an effective segmentation model [33]. However, it’s unclear whether the features are easily separable using unsupervised methods.

We examined the applicability of three definitions for $m(p)$: DINOv2 embedding, mean RGB color, and patch position. To produce the final DINO embeddings, images were resized to $14d \times 14d$, such that each GraPL patch corresponds to a 14×14 DINO patch. These embeddings were reduced to K_0 dimensions using 2nd degree polynomial PCA. As a baseline, we also tested a version where the fully connected graph was replaced with a 4-neighborhood lattice of uniformly weighted edges.

In our tests, DINOv2 embeddings were a significantly better metric than distance alone (Table 2). However, they were outperformed by simple RGB color vectors. Acknowledging DINOv2’s ability to act as a feature extractor for supervised segmentation, further research is needed to determine what types of transformations are necessary for converting the embeddings into a better affinity metric.

Initializer	mIoU
Patchwise Rand.	0.496
Seedwise Rand.	0.507
Spatial	0.509
SLIC	0.512

Table 1. Comparison of pseudo-label initialization methods

Metric	mIoU
Uniform	0.459
Position	0.476
Color	0.527
DINOv2	0.512

Table 2. Comparison of pairwise weighting metrics

Warm Start GraPL is designed to train the same network continuously throughout all iterations. This is in contrast to similar iterative methods which prefer a “cold start,” re-initializing the parameters of the surrogate function prior to subsequent iterations. Preliminary tests showed that in our case, a “warm start” approach is preferred to re-initializing the network each time. These two approaches in fact produce very different loss curves (Figure 3). Cold starts produce large spikes in loss at the beginning of each training iteration, whereas warm starts require only minor adjustments at these points. We expect that the first iterations of training provide important feature learning to the first lay-

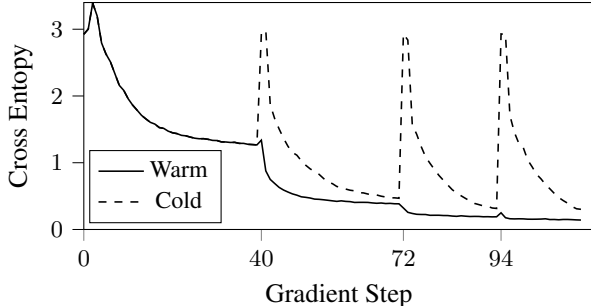


Figure 3. Comparison of loss curves using warm and cold starting methods, averaged over all test images in BSDS500 [3]. Here we consider the loss value at the end of each gradient step. On the x-axis, we depict the instants where a new training iteration starts.

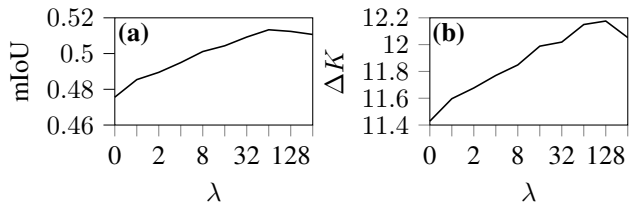


Figure 4. Effects of pairwise energy coefficient. (a) Effect of λ on mIoU. (b) Effect of λ on ΔK .

ers of the network. By starting cold at each iteration, subsequent iterations are unable to benefit from the learned low-level feature detectors and therefore present a more unstable training phase.

Pairwise Energy Coefficient (λ) GraPL uses graph cuts to generate each new set of pseudo-labels, working on the theory that this graphical representation of the image provides an important spatial coherence prior, which is perhaps missing from similar unsupervised methods, and accounts for its success. Furthermore, GraPL relies on pairwise costs as well as the continuity loss to gradually decrease \hat{K} . To test these ideas, we evaluated the segmentation performance of the algorithm as well as ΔK across different values of λ , the hyperparameter which defines the scale of the pairwise energy as defined in Eq. 4.

When $\lambda = 0$, cutting any non-terminal edge incurs no cost. In this case, the function of the cut is effectively the same as the argmax clustering step found in [25], as pseudo-labels are entirely dependent on the current network response vectors. As λ increases, network response vectors are made less influential in the pseudo-label assignment process, as expected.

The results in Figure 4 demonstrate a logarithmic increase in segmentation performance as λ is raised from 0 through 64. However, increasing λ to values higher than 64 tends to result in comparatively poor performance. Because

increasing λ strengthens pairwise connections, we would expect it to be closely correlated with ΔK . When $\lambda \leq 64$, we observe this behavior; however, higher values actually result in a plateau or slight decrease in ΔK .

In a configuration where the pairwise edges were uniformly weighted (or weighted according to spatial distance), we would expect higher than optimal values of λ to push ΔK too high and produce oversimplified segmentations, where multiple target segments are collapsed into a single predicted segment. However, when pairwise edges are weighted by patch encoder embedding affinity, pushing λ too high can instead result in an overly detailed segmentation, in which the graph cut considers the pairwise energy (dictated by the patch embeddings) more than the unary weights learned by GraPL.

Continuity Loss Spatial continuity loss, first introduced in [25], provides GraPL a spatial coherence prior which penalizes the network directly at each gradient step, rather than through the graph cut produced pseudo-labels at the end of each iteration. Though shown effective in [25], we instinctively believed that it would be redundant in a graphically guided pipeline like GraPL. However, we observed that the combination of the two different spatial coherence priors produced more accurate segmentations than either one alone (Figure 5).

In practice, we noted that this loss has a different mechanism of action than the graphical coherence prior. In the absence of this spatial loss, GraPL employs a level of trust in the patch encoder that may be unfounded, as the pairwise energy only penalizes the separation of patches with a great affinity; but when using a patch encoder like DINO, which is defined by a large neural network, the edge weights may be high variance. In this case, increasing λ only serves to emphasize the patch encoder’s bias for certain edges. However, increasing the weight of the spatial continuity loss applies a higher penalty for *all* edges. In effect, it could be compared to an additive bias term in the pairwise energy function that raises the cost, no matter the patch affinity.

Patch Size Patch-based approaches are faced with a choice between granularity (with smaller patches) and the information richness of input (with larger patches). In GraPL’s case, smaller patches also entail more complex

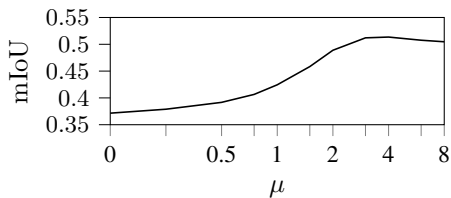


Figure 5. Effect of spatial continuity loss weight on mIoU

graphs that take longer to solve, and larger patches entail higher memory usage. We found that setting d equal to 32 offered both optimal performance and near optimal efficiency (Table 3).

d	mIoU	Seconds per Image
8	0.248	3.49
16	0.372	1.72
32	0.512	1.75
64	0.496	6.98

Table 3. mIoU and segmentation time as a function of patch size. Time measurements are based on segmentation of BSDS500 test set on an Nvidia A100 GPU and AMD Epyc 7343 CPU.

4.3. Comparison to Other Methods

We compared the segmentation performance of GraPL to six other unsupervised deep-learning methods: Differentiable Feature Clustering (DFC) [25], Invariant Information Clustering (IIC) [24], Pixel-level feature Clustering using Invariance and Equivariance (PiCIE) [15], Segment Sorting (SegSort) [23] and W-Net [45]. We also tested two baselines which use SLIC to segment images based on RGB and DINOv2 [33] patch embeddings (interpolated to the pixel level). These baselines were selected to demonstrate that the success of our method does not simply originate from its initialization or its pretrained guidance. PiCIE and SegSort were trained on their preferred datasets, COCO-Stuff [8] and PASCAL VOC 2012 [17], as BSDS500 is too small, while the others used only BSDS500.

Table 4 summarizes the quantitative comparative results of the above methods, where segmentation performance was measured in terms of both mIoU and pixel accuracy [19]. As with mIoU, pixel accuracy was computed using a one-to-one label matching strategy. Figure 6 displays some segmentation results from the above methods for qualitative comparison.

Compared to other unsupervised methods, GraPL is able to decompose complex foregrounds into detailed yet semantically salient components. Notice how GraPL is able to pick up on small details like sunglasses in the distance while ignoring less relevant features of the image, such as creases in clothing. In many cases, it is able to handle color gradient variation, usually present in sky backgrounds or shadow regions. On occasion, GraPL detects segments that are not present in the ground-truth, such as the bird heads on the last qualitative example, which, despite being reasonable, decreases its quantitative performance. Finally, it also struggles to detect fine structures, such as castle tops, small holes and bird beaks. Despite that, our proposed method is able to outperform all of the compared methods by a margin of at least 6.9% in accuracy and 9.3% mIoU. It is also worth



Figure 6. Qualitative comparison of GraPL to other deep learning-based unsupervised segmentation methods. We selected two of the available ground truth segmentations (GT1 and GT2) for comparison, one more detailed and one less detailed.

Method	mIoU	Accuracy
SLIC (RGB features)	0.137	0.416
SLIC (DINOv2 features)	0.258	0.280
DFC [25]	0.398	0.505
DoubleDIP [18]	0.356	0.423
IIC [24]†	0.172	
PiCIE [15]	0.325	0.405
SegSort [23]	0.480	0.505
W-Net [45]	0.428	0.531
GraPL (proposed)	0.527	0.569

Table 4. BSDS500 performance comparison of GraPL with other unsupervised deep-learning methods and baselines.

†The value listed for IIC is sourced from [25].

noting the low performance of our baselines, when compared to GraPL. This demonstrates that our method does not merely rest on the success of our our initializer, SLIC. Instead, GraPL’s success is a product of its novel training and inference methodology.

5. Conclusion

In this paper, we introduce GraPL, a deep learning-based unsupervised segmentation framework that approaches the problem by solving a patch clustering surrogate task to learn network parameters which are then used for pixel-level classification. Additionally, GraPL is the first deep learning method to employ a graph cut regularizer during training, which encourages spacial coherence and leverages the discriminative power of patch embeddings. Furthermore, it seamlessly translates patch-level learning to the pixel-level without the need for postprocessing. Our experiments demonstrate our algorithm’s promising capacities, as it is able to outperform many state-of-the-art unsupervised segmentation methods. Our work can be seen as further evidence for the benefit of using graph cuts in deep learning, especially in the context of unsupervised segmentation.

References

- [1] Kenneth Abend, TI Harley, and L Kanal. Classification of binary random patterns. *IEEE Transactions on Information Theory*, 11(4):538–544, 1965. 2

- [2] Radhakrishna Achanta, Appu Shaji, Kevin Smith, Aurelien Lucchi, Pascal Fua, and Sabine Süsstrunk. Slic superpixels compared to state-of-the-art superpixel methods. *IEEE Transactions on Pattern Analysis and Machine Intelligence*, 34(11):2274–2282, 2012. 5
- [3] Pablo Arbelaez, Michael Maire, Charless Fowlkes, and Jitendra Malik. Contour detection and hierarchical image segmentation. *IEEE Trans. Pattern Anal. Mach. Intell.*, 33(5):898–916, May 2011. 5, 6
- [4] Ismail Ben Ayed, Hua-mei Chen, Kumaradevan Punithakumar, Ian Ross, and Shuo Li. Graph cut segmentation with a global constraint: Recovering region distribution via a bound of the bhattacharyya measure. In *2010 IEEE Computer Society Conference on Computer Vision and Pattern Recognition*, pages 3288–3295. IEEE, 2010. 4
- [5] Julian Besag. On the statistical analysis of dirty pictures. *Journal of the Royal Statistical Society Series B: Statistical Methodology*, 48(3):259–279, 1986. 2
- [6] Yuri Boykov, Olga Veksler, and Ramin Zabih. Fast approximate energy minimization via graph cuts. *IEEE Transactions on pattern analysis and machine intelligence*, 23(11):1222–1239, 2001. 2, 3, 4
- [7] Yuri Y Boykov and M-P Jolly. Interactive graph cuts for optimal boundary & region segmentation of objects in nd images. In *Proceedings eighth IEEE international conference on computer vision. ICCV 2001*, volume 1, pages 105–112. IEEE, 2001. 1, 2, 3
- [8] Holger Caesar, Jasper Uijlings, and Vittorio Ferrari. Coco-stuff: Thing and stuff classes in context. In *Computer vision and pattern recognition (CVPR), 2018 IEEE conference on*. IEEE, 2018. 7
- [9] Nicolas Carion, Francisco Massa, Gabriel Synnaeve, Nicolas Usunier, Alexander Kirillov, and Sergey Zagoruyko. End-to-end object detection with transformers. In *European conference on computer vision*, pages 213–229. Springer, 2020. 1
- [10] Mathilde Caron, Piotr Bojanowski, Armand Joulin, and Matthijs Douze. Deep clustering for unsupervised learning of visual features. In *Proceedings of the European conference on computer vision (ECCV)*, pages 132–149, 2018. 4, 5
- [11] Mathilde Caron, Hugo Touvron, Ishan Misra, Hervé Jégou, Julien Mairal, Piotr Bojanowski, and Armand Joulin. Emerging properties in self-supervised vision transformers. In *Proceedings of the IEEE/CVF international conference on computer vision*, pages 9650–9660, 2021. 1, 2
- [12] Tony F Chan and Luminita A Vese. Active contours without edges. *IEEE Transactions on image processing*, 10(2):266–277, 2001. 1
- [13] Liang-Chieh Chen, George Papandreou, Iasonas Kokkinos, Kevin Murphy, and Alan L Yuille. Deeplab: Semantic image segmentation with deep convolutional nets, atrous convolution, and fully connected crfs. *IEEE transactions on pattern analysis and machine intelligence*, 40(4):834–848, 2017. 1, 2
- [14] Liang-Chieh Chen, George Papandreou, Florian Schroff, and Hartwig Adam. Rethinking atrous convolution for semantic image segmentation. *arXiv preprint arXiv:1706.05587*, 2017. 2
- [15] Jang Hyun Cho, Utkarsh Mall, Kavita Bala, and Bharath Hariharan. Picie: Unsupervised semantic segmentation using invariance and equivariance in clustering. In *Proceedings of the IEEE/CVF Conference on Computer Vision and Pattern Recognition*, pages 16794–16804, 2021. 2, 7, 8
- [16] Noha Youssry El-Zehiry and Leo Grady. Fast global optimization of curvature. In *2010 IEEE Computer Society Conference on Computer Vision and Pattern Recognition*, pages 3257–3264. IEEE, 2010. 4
- [17] M. Everingham, L. Van Gool, C. K. I. Williams, J. Winn, and A. Zisserman. The PASCAL Visual Object Classes Challenge 2012 (VOC2012) Results. <http://www.pascal-network.org/challenges/VOC/voc2012/workshop/index.html>. 7
- [18] Yosef Gandelsman, Assaf Shocher, and Michal Irani. ”double-dip”: unsupervised image decomposition via coupled deep-image-priors. In *Proceedings of the IEEE/CVF Conference on Computer Vision and Pattern Recognition*, pages 11026–11035, 2019. 8
- [19] Alberto Garcia-Garcia, Sergio Orts-Escolano, Sergiu Oprea, Victor Villena-Martinez, and Jose Garcia-Rodriguez. A review on deep learning techniques applied to semantic segmentation, 2017. 5, 7
- [20] Mark Hamilton, Zhoutong Zhang, Bharath Hariharan, Noah Snavely, and William T Freeman. Unsupervised semantic segmentation by distilling feature correspondences. In *International Conference on Learning Representations*, 2021. 1
- [21] Mark Hamilton, Zhoutong Zhang, Bharath Hariharan, Noah Snavely, and William T Freeman. Unsupervised semantic segmentation by distilling feature correspondences. *arXiv preprint arXiv:2203.08414*, 2022. 1, 2, 4
- [22] Kai Han, Yunhe Wang, Jianyuan Guo, Yehui Tang, and Enhua Wu. Vision gnn: An image is worth graph of nodes. *Advances in Neural Information Processing Systems*, 35:8291–8303, 2022. 1
- [23] Jyh-Jing Hwang, Stella X Yu, Jianbo Shi, Maxwell D Collins, Tien-Ju Yang, Xiao Zhang, and Liang-Chieh Chen. Segsort: Segmentation by discriminative sorting of segments. In *Proceedings of the IEEE/CVF International Conference on Computer Vision*, pages 7334–7344, 2019. 2, 4, 7, 8
- [24] Xu Ji, Joao F Henriques, and Andrea Vedaldi. Invariant information clustering for unsupervised image classification and segmentation. In *Proceedings of the IEEE/CVF international conference on computer vision*, pages 9865–9874, 2019. 2, 3, 7, 8
- [25] Wonjik Kim, Asako Kanezaki, and Masayuki Tanaka. Unsupervised learning of image segmentation based on differentiable feature clustering. *IEEE Transactions on Image Processing*, 29:8055–8068, 2020. 1, 2, 3, 4, 5, 6, 7, 8
- [26] Vladimir Kolmogorov and Yuri Boykov. What metrics can be approximated by geo-cuts, or global optimization of length/area and flux. In *Tenth IEEE International Conference on Computer Vision (ICCV’05) Volume 1*, volume 1, pages 564–571. IEEE, 2005. 4
- [27] Philipp Krähenbühl and Vladlen Koltun. Efficient inference in fully connected crfs with gaussian edge potentials. *Ad-*

- vances in neural information processing systems*, 24, 2011. **1**
- [28] Stan Z Li. *Markov random field modeling in image analysis*. Springer Science & Business Media, 2009. **2**
- [29] Yujia Li and Jirka Borovec. pygco. <https://github.com/Borda/pyGCO>, 2023. **5**
- [30] Qinghong Lin, Weichan Zhong, and Jianglin Lu. Deep superpixel cut for unsupervised image segmentation. In *2020 25th International Conference on Pattern Recognition (ICPR)*, pages 8870–8876. IEEE, 2021. **1**
- [31] Dmitrii Marin, Meng Tang, Ismail Ben Ayed, and Yuri Boykov. Beyond gradient descent for regularized segmentation losses. In *Proceedings of the IEEE/CVF Conference on Computer Vision and Pattern Recognition*, pages 10187–10196, 2019. **2**
- [32] Shervin Minaee, Yuri Boykov, Fatih Porikli, Antonio Plaza, Nasser Kehtarnavaz, and Demetri Terzopoulos. Image segmentation using deep learning: A survey. *IEEE transactions on pattern analysis and machine intelligence*, 44(7):3523–3542, 2021. **1**
- [33] Maxime Oquab, Timothée Darcet, Théo Moutakanni, Huy Vo, Marc Szafraniec, Vasil Khalidov, Pierre Fernandez, Daniel Haziza, Francisco Massa, Alaaeldin El-Nouby, et al. Dinov2: Learning robust visual features without supervision. *arXiv preprint arXiv:2304.07193*, 2023. **2, 5, 6, 7**
- [34] Yassine Ouali, Céline Hudelot, and Myriam Tami. Autoregressive unsupervised image segmentation. In *Computer Vision—ECCV 2020: 16th European Conference, Glasgow, UK, August 23–28, 2020, Proceedings, Part VII 16*, pages 142–158. Springer, 2020. **3**
- [35] Adam Paszke, Sam Gross, Francisco Massa, Adam Lerer, James Bradbury, Gregory Chanan, Trevor Killeen, Zeming Lin, Natalia Gimelshein, Luca Antiga, Alban Desmaison, Andreas Kopf, Edward Yang, Zachary DeVito, Martin Raison, Alykhan Tejani, Sasank Chilamkurthy, Benoit Steiner, Lu Fang, Junjie Bai, and Soumith Chintala. PyTorch: An Imperative Style, High-Performance Deep Learning Library. In H. Wallach, H. Larochelle, A. Beygelzimer, F. d’Alché Buc, E. Fox, and R. Garnett, editors, *Advances in Neural Information Processing Systems 32*, pages 8024–8035. Curran Associates, Inc., 2019. **5**
- [36] Yazhou Ren, Jingyu Pu, Zhimeng Yang, Jie Xu, Guofeng Li, Xiaorong Pu, Philip S Yu, and Lifang He. Deep clustering: A comprehensive survey. *arXiv preprint arXiv:2210.04142*, 2022. **1, 2**
- [37] Olaf Ronneberger, Philipp Fischer, and Thomas Brox. U-net: Convolutional networks for biomedical image segmentation. In *Medical Image Computing and Computer-Assisted Intervention—MICCAI 2015: 18th International Conference, Munich, Germany, October 5–9, 2015, Proceedings, Part III 18*, pages 234–241. Springer, 2015. **1**
- [38] Carsten Rother, Vladimir Kolmogorov, and Andrew Blake. ” grabcut” interactive foreground extraction using iterated graph cuts. *ACM transactions on graphics (TOG)*, 23(3):309–314, 2004. **2, 3**
- [39] Jianbo Shi and Jitendra Malik. Normalized cuts and image segmentation. *IEEE Transactions on pattern analysis and machine intelligence*, 22(8):888–905, 2000. **1**
- [40] Meng Tang, Lena Gorelick, Olga Veksler, and Yuri Boykov. Grabcut in one cut. In *Proceedings of the IEEE international conference on computer vision*, pages 1769–1776, 2013. **4**
- [41] Ilya O Tolstikhin, Neil Houlsby, Alexander Kolesnikov, Lucas Beyer, Xiaohua Zhai, Thomas Unterthiner, Jessica Yung, Andreas Steiner, Daniel Keysers, Jakob Uszkoreit, et al. Mlp-mixer: An all-mlp architecture for vision. *Advances in neural information processing systems*, 34:24261–24272, 2021. **1**
- [42] Asher Trockman and J Zico Kolter. Patches are all you need? *arXiv preprint arXiv:2201.09792*, 2022. **1**
- [43] Xudong Wang, Rohit Girdhar, Stella X Yu, and Ishan Misra. Cut and learn for unsupervised object detection and instance segmentation. In *Proceedings of the IEEE/CVF Conference on Computer Vision and Pattern Recognition*, pages 3124–3134, 2023. **2, 3, 4**
- [44] Yangtao Wang, Xi Shen, Yuan Yuan, Yuming Du, Maomao Li, Shell Xu Hu, James L Crowley, and Dominique Vaufreydaz. Tokencut: Segmenting objects in images and videos with self-supervised transformer and normalized cut. *arXiv preprint arXiv:2209.00383*, 2022. **1, 2, 3, 4**
- [45] Xide Xia and Brian Kulis. W-net: A deep model for fully unsupervised image segmentation. *arXiv preprint arXiv:1711.08506*, 2017. **7, 8**
- [46] Enze Xie, Wenhai Wang, Zhiding Yu, Anima Anandkumar, Jose M Alvarez, and Ping Luo. Segformer: Simple and efficient design for semantic segmentation with transformers. *Advances in Neural Information Processing Systems*, 34:12077–12090, 2021. **1**
- [47] Hongshan Yu, Zhengeng Yang, Lei Tan, Yaonan Wang, Wei Sun, Mingui Sun, and Yandong Tang. Methods and datasets on semantic segmentation: A review. *Neurocomputing*, 304:82–103, 2018. **1**
- [48] Shuai Zheng, Sadeep Jayasumana, Bernardino Romera-Paredes, Vibhav Vineet, Zhizhong Su, Dalong Du, Chang Huang, and Philip HS Torr. Conditional random fields as recurrent neural networks. In *Proceedings of the IEEE international conference on computer vision*, pages 1529–1537, 2015. **2**